

Predicting the Mpemba Effect Using Machine Learning

Felipe Amorim,^{1,*} Joey Wisely,^{1,†} Nathan Buckley,^{1,‡} Christiana DiNardo,^{1,§} and Daniel Sadasivan^{1,¶}

¹*Ave Maria University, Ave Maria, FL 34142, USA*

The Mpemba Effect – when a system that is further from equilibrium relaxes faster than a system that is closer – can be studied with Markovian dynamics in a non-equilibrium thermodynamics framework. The Markovian Mpemba Effect can be observed in a variety of systems including the Ising model. We demonstrate that the Markovian Mpemba Effect can be predicted in the Ising model with several machine learning methods: the decision tree algorithm, neural networks, linear regression, and non-linear regression with the LASSO method. The effectiveness of these methods are compared. Additionally, we find that machine learning methods can be used to accurately extrapolate to data outside the range which they were trained. Neural Networks can even predict the existence of the Mpemba Effect when they are trained only on data in which the Mpemba Effect does not occur. This indicates that information about the effect is contained even in systems where it is not present. All of these results demonstrate that the Mpemba Effect can be predicted in complex, computationally expensive systems, without performing full calculations.

I. INTRODUCTION

A. Mpemba Effect

The Mpemba Effect involves two systems that are not in equilibrium. It occurs when the system that is initially farther from equilibrium becomes closer to equilibrium. The best known example is the claim that hot water can freeze faster than cool water in the same environment. This was named after Erasto Mpemba, who most famously brought it to the attention of the scientific community [1] although it has been debated for thousands of years [2–4].

Several recent theoretical explanations of the effect have been demonstrated. One shows that the Mpemba Effect can be predicted from statistical mechanics [5–9]. Another explanation, Refs. [10, 11] makes use of the framework developed in Ref. [10], which considers the Markovian dynamics as cooling process in the framework of non-equilibrium thermodynamics. We refer to this process as the Markovian Mpemba Effect (MME). The MME is further studied in Refs. [12, 13] Ref. [10] applies the MME to an antiferromagnetic nearest-neighbor interacting Ising spin chain, generalizing the Mpemba Effect to other systems. The one-dimensional Ising spin chain will be the main model used in this paper, enabling us to use machine learning methods to predict the effect, as described in Sec. II.

The Mpemba Effect traditionally describes systems relaxing towards an equilibrium temperature that is lower than their initial temperature. However, a reverse effect occurs when two systems relax towards equilibrium at a higher temperature. Sometimes the former is referred to

as the Mpemba Effect and the latter is referred to as the Inverse Mpemba Effect, but both cases meet the definition of the Mpemba Effect used in this paper, namely that the system that is initially farther from equilibrium becomes closer after a finite time. Unless otherwise specified we refer to the Inverse Markovian Mpemba Effect simply as the Mpemba Effect.

This paper is organized as follows. Sec. IB discusses recent works with results that can be related to our results. Sec. II, describe the formalism (laid out by Ref. [10, 11]) used to determine the Mpemba Effect in the Ising model. Sec. III, summarizes the various machine learning methods employed. The main results of this work are presented and discussed in Sec. IV. We conclude in Sec. V.

B. Applications and Impact

The Mpemba Effect has been observed in a number of systems. In addition to water, [14, 15], it has been predicted in magnetoresistance alloys [16], numerically predicted in colloids [17], predicted analytically and numerically in gasses [18, 19], predicted in particles bounded by anharmonic potentials [20], observed in computational simulations and experiments in gas hydrates [21], and in computational simulations of carbon nanotube resonators [22]. It has been demonstrated to have application for faster heating with precooling [23], that the effect happens for temperatures dependent on the maximum work that can be extracted from the system [24], and that the Mpemba Effect can lead to quantum heat engines with greater power output and stability [25].

Furthermore, the Mpemba Effect is closely linked to the Kovacs Memory Effect, by which systems out of equilibrium cannot merely be described by macroscopic thermodynamic variables. Knowledge of the Mpemba Effect can be applied when studying memory effects in Refs. [26–30].

These works demonstrate the potential applications of the effect and motivate better statistical understanding. To our knowledge, no work has used machine methods to

* FelipeAugusto.deAmor@my.avemaria.edu

† Peter.Wisely@my.avemaria.edu

‡ Nathan.Buckley@my.avemaria.edu

§ Christiana.George@my.avemaria.edu

¶ Daniel.Sadasivan@avemaria.edu

predict the occurrence of the ME in any system. The work presented in this paper uses learning methods to predict the Mpemba Effect in the Ising model. The comparison of methods done in this analysis could be applied to the prediction of the ME in other systems.

Machine learning has previously been applied to the Ising model in a number of ways other than the Mpemba Effect: using autoencoding neural networks, [31], using neural networks [32] to predict probability distribution, and comparison of various classification methods such as random forests, decision trees, k nearest neighbors and artificial neural networks [33].

These works find several interesting results that can be compared to the work in this paper. Firstly, Ref. [32] found that only the number of nodes in the first layer of the deep neural network could improve the accuracy of the prediction. Secondly, Ref. [33] found that the Decision Tree method was the most accurate predictor. Even though previous results predict different things, comparison with our work could show general trends in machine learning applied to the Ising model.

II. THE MARKOVIAN MPEMBA EFFECT FORMALISM

This work uses the formalism developed in Refs. [10, 11] for the Mpemba Effect in the Ising model. We summarize the key equations in the following.

The one-dimensional Ising model consists of a chain of N spins, s_i with values of 1 or -1. The energy for a given set of spins is defined to be

$$E = -J \sum_{k=0}^N s_k s_{k+1} - h \sum_{k=1}^N s_k, \quad (1)$$

where J and h are parameters respectively giving the field of interaction between neighboring spins and the strength of the external field.

A probabilistic distribution $\vec{p}(t)$ that represents the probability of finding the system in one of the 2^N micro-states is defined for the case of a finite number of states, by the equation:

$$\frac{d\vec{p}(t)}{dt} = R(T_b)\vec{p}(t), \quad (2)$$

for $i = 1, 2, \dots, n$. Matrix multiplication is assumed. Here $R_{ij}(T_b)$ is the transition rate matrix from a state j to state i defined as:

$$R_{ij} = \begin{cases} \Gamma e^{-\frac{1}{2}\beta_b(E_i - E_j)}, & \text{if } i \text{ and } j \text{ differ by one spin flip} \\ 0, & \text{if } i \text{ and } j \text{ differ by } > 1 \text{ spin flip} \\ -\sum_{k \neq j} R_{kj}, & i = j \end{cases} \quad (3)$$

At a given temperature, a system will have an equilibrium state,

$$\vec{\pi}(T) = \frac{e^{-E_i/k_B T}}{\sum_i e^{-E_i/k_B T}}. \quad (4)$$

Because the eigenvalues form a complete basis, any state can be expressed as,

$$\vec{p} = \vec{\pi}(T) + \sum_{i>1} a_i \vec{v}_i \quad (5)$$

where v_i are the eigenvectors of the rate transition matrix and a_i are coefficients. $\vec{\pi}$ is the eigenvector corresponding to an eigenvalue of 0.

The general solution to Eq. (2) is given by

$$\vec{p}(T; t) = e^{Rt} \vec{\pi}(T) = \vec{\pi}(T_b) + \sum_{i>1} a_i(T) e^{\lambda_i t} \vec{v}_i, \quad (6)$$

and λ_i are the eigenvalues of the transition rate matrix.

The distance from equilibrium function, $D[\vec{p}(t); T_b]$, is given by

$$D[\vec{p}(t); T_b] = \sum_i \left(\frac{E_i(p_i - \pi_i^b)}{T_b} + p_i \ln p_i - \pi_i^b \ln \pi_i^b \right). \quad (7)$$

The Mpemba Effect occurs for any two probability distributions \vec{p}_H and \vec{p}_C if $D[\vec{p}_H(0); T_b] > D[\vec{p}_C(0); T_b]$ but $D[\vec{p}_H(t'); T_b] < D[\vec{p}_C(t'); T_b]$ for some time, t' . Ref. [10] shows that this will occur if $|a_2^H| < |a_2^C|$.

III. MACHINE LEARNING METHODS

The data used for the various machine learning methods is generated in the following way. The matrix R_{ij} , given in Eq. (3), is calculated for a given J , h , T , and N . Sparse Matrix methods are used to improve the speed of the computation. The Arnoldi method [34] is used to calculate the second greatest (least negative) eigenvalue and the corresponding eigenvector. These correspond to λ_2 and \vec{v}_2 from Eq. (6). These can be used to calculate a_2 using the method described of Sec. II in Ref. [11].

We use four different machine learning methods to predict the occurrence of the Mpemba Effect in an Ising chain between 5 and 15 spins. We work only with odd-numbered spins because these have different equilibria for the anti-ferromagnetic Ising model. All of these methods have certain free parameters called fit parameters and a loss function which measures the distance of the prediction from the data. The methods use various algorithms to fit the data or match the model to the data.

A. Decision Tree Algorithm (DT)

For the decision tree, the classification of data is divided into two classes: for each set of initial conditions, the system can either undergo the IMME or not. We use a data set with in the format of:

$$\{N, J, h, T_c, T_h\} = \begin{cases} 1 & \text{if IMME occurs} \\ 0 & \text{if IMME does not occur,} \end{cases} \quad (8)$$

The decision tree is trained using the CART (Classification And Regression Tree) algorithm [35]. This algorithm uses a flow chart-style tree to classify the input and predict output. Because this method minimizes a loss function different from the other methods we use, we do not record any loss function.

B. Neural Network (NN)

Neural networks can be trained to predict the parameters $|a_2|$ given a set of Mpemba parameters. Prediction of a_2 is sufficient to determine whether the Mpemba Effect occurs. The network is trained on 4 input parameters,

$$\{N, J, h, T\} = |a_2| \quad (9)$$

Note that we multiply each $|a_2|$ by 10000, to make the values a more natural size. This has no impact on the mathematics of prediction for the neural network or any other machine learning method, however, many algorithms are built to select initial values that are more naturally sized. This adjustment prevents the need to change the starting parameters of each algorithm.

We find the most accurate neural network consists of 3 hidden layers with 50, 20, and 5 nodes respectively. Each layer as well as the output layer uses the Scaled Exponential Linear Unit (SELU) activation function. The loss function is the Mean Squared Logarithmic Error (MSLE) [36]. This is given with the formula

$$L(y, \hat{y}) = \frac{1}{n} \sum_{i=0}^n (\log(y_i + 1) - \log(\hat{y}_i + 1))^2, \quad (10)$$

where y_i are the actual values, n is the number of data points, and \hat{y}_i are the predicted values.

The neural network can also be used to directly predict the Mpemba Effect rather than predicting $|a_2|$. This is done by training the network with data given by Eq. (8). The network remains the same except that the output layer has a sigmoid activation function and a binary cross-entropy loss function is used. The case where the Mpemba Effect is predicted directly is referred to as NN2.

C. Linear Regression (LR)

Linear regression is used to predict the $|a_2|$ coefficients with the data. We once again minimize the MSLE given

	c_0	N	J	h	T
Regression coefficients	10.191	84.359	-78.725	-9.889	-36.903
Correlation coefficients	-	-0.005	-0.370	-0.027	-0.601

TABLE I. Upper Row: The linear regression fit parameters. The parameter in column i corresponds to the fit parameters c_i in Eq. (11). The first column is labeled c_0 . The other columns are labeled with the parameters that c_i is multiplied by. Lower Row: The correlation coefficients between each parameter and a_2 .

in Eq. (10). The predicted values, \hat{y}_i , are given by

$$\hat{y}_i = \sum_{j=0}^4 c_j x_{ij}. \quad (11)$$

$$x_{i0} = 1; \quad x_{i1} = N; \quad x_{i2} = J; \quad x_{i3} = h; \quad x_{i4} = T_i.$$

The fit parameters are c_j .

The MSLE is chosen as the loss function rather than the sum of least squares because it more accurately captures the behavior of data with very different orders of magnitude.

Linear regression cannot be used to determine the Mpemba Effect because, for the effect to occur, $|a_2|$ must increase as T increases. If $|a_2|$ is given by a decreasing linear function of T , the T that is farther from equilibrium will always correspond to a larger value of $|a_2|$. This can be seen in the linear fit in Fig. 3.

Nevertheless, linear regression is useful for two reasons. Firstly, the MSLE can be compared to other methods, giving information about their accuracy. Secondly, the values of the fit parameters c_j can be used as a crude approximation of the importance of each category of data for predicting $|a_2|$.

The fit parameters are given in Tab. I. We also quote the correlation coefficients which correspond to an even simpler model. Note that because the linear regression in the fit was performed by minimizing the MSLE rather than the least squares, ordinary relations between correlation coefficients and linear fit parameters do not apply.

D. Nonlinear Regression (NLR) with the LASSO Method

The data can be more accurately described with a nonlinear model. We use a general expansion of the form

$$\hat{y}_i = \sum_{k_1=0}^N \cdots \sum_{k_n=0}^N \delta_{N, \sum_i k_i} c_{k_1 \dots k_N} \prod_{j=1}^4 P_{k_j}(x_{ij}) \quad (12)$$

where $P_{k_j}(x_{ij})$ are the Legendre Polynomials mapped to the range of each data set, N is the order up to which we

consider, $\delta_{N, \sum_i k_i}$ is the Kronecker Delta Function, and $c_{k_1 \dots k_N}$ are the fit parameters. In the case when $N = 1$, this expansion reduces to linear regression. The error minimized is once again the MSLE given in Eq. (10).

For large N , the number of fit parameters lead to a prohibitive computational cost of the minimization. Not all fit parameters at a given order are equally effective at minimization. The LASSO Method [37–40] is employed in order to determine which fit parameters are most effective and which can be neglected to reduce computational cost. This is done in the following way. We randomly select 1000 data points and use them to calculate a modified loss function given by

$$L(y, \hat{y}) = \frac{1}{n} \sum_{i=0}^n (\log(y_i + 1) - \log(\hat{y} + 1))^2 + \lambda \sum |c_{ijkl}|. \quad (13)$$

The term λ is a penalty term that can be varied. The data points are used to find the fit parameters that lead to local minima for various values of λ . When $\lambda = 0$, all fit parameters are non-zero. As λ becomes large, all fit parameters approach 0. A number of fits are performed with all fit parameters up to the fourth order with a gradually increasing λ . The fit parameters are ranked according to the value of λ necessary to reach an absolute value less than 10^{-6} . This list is ordered in terms of importance for the minimization of the MSLE. A visualization of the ordering can be found in Fig. 1 which shows the values of the second order parameters as λ is increased. The lower the value of λ at which the parameters are close to 0, the less important they are.

The parameters are then validated by calculating the MSLE with new data. First the data are validated with a fit involving all parameters. Next, the same validation is performed while excluding the parameter determined to

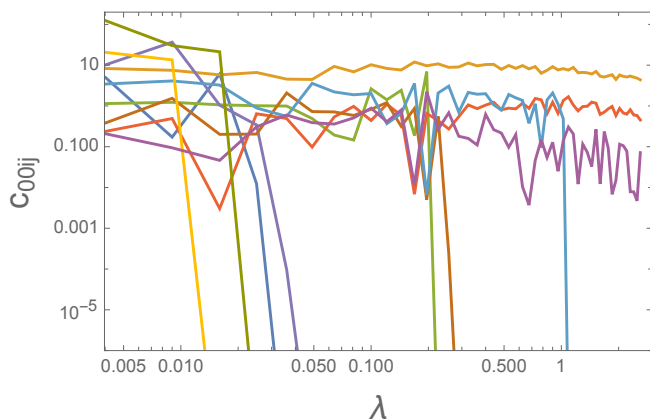


FIG. 1. The best fit values of parameters c_{00ij} for i and j from 1 to 4 defined in Eq. (12). The parameters are obtained by minimizing the loss function given in Eq. (13) for various λ . As λ increases, c_{00ij} will become small. The order in which the parameters approach 0 gives the order of importance of each parameter in minimizing the MSLE.

be least important. After that, the least important two parameters are excluded. This process continues until all parameters have been excluded. This process generates a list of validation MSLE with parameters excluded in order of importance from least important to most important. The validation MSLE is plotted in Fig. 2.

The plot shows a minimum when 22 parameters are excluded. Thus 22 parameters are excluded for the non-linear regression. This allows for quicker minimization.

When fitting the data the following procedure is performed. Firstly, we fit the parameters c_{000i} to the data from i from 0 to 4 using the Newton method. The other fit parameters are kept constant at 0. Next we fit the parameters c_{00ij} with i and j from 0 to 4. The initial values of c_{000i} are the best fit values from the previous minimization. The other fit parameters are given initial values 0. All parameters not used in the fit are once again set to 0. The same process is repeated for c_{0ijk} , and finally for c_{ijkl} .

This method of finding minimum parameters is employed in order to find a stable local minimum. If all parameters were fitted at once without appropriate starting values, small changes in the fit such as changing the number of data points or increasing the penalty term would result in drastically different local minima. However, it causes the fit to rely most heavily on lower order parameters.

The best fit parameters are given in Tab. VI in the Appendix. Perhaps because of the fit procedure, far more higher order parameters than lower order parameters are found by the LASSO to be unnecessary.

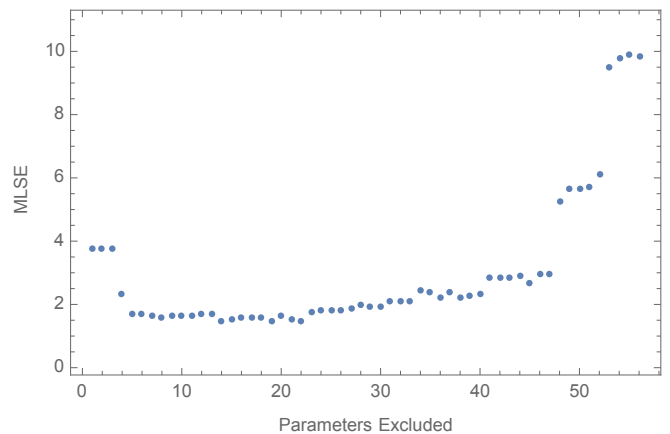


FIG. 2. The validation MSLE varying the number of excluded parameters. The data were fit to 1000 training points. The parameters are excluded in order of impact as described in the text. The minimum corresponds to a number of excluded parameters that neither overfit nor underfit the 1000 data points.

IV. RESULTS AND DISCUSSION

A. Comparison of Methods

An example of the various methods compared with the data is shown in Fig. 3. Only the methods that predict $|a_2|$ directly are shown. The black dots give the actual computed data. At very low temperatures, they increase slightly with temperature indicating a very weak Mpemba Effect. After that, they decrease smoothly to equilibrium.

In order to compare the effectiveness of the various methods, several metrics are used. All of these metrics distinguish between training data, which are used to fix the free parameters or nodes of the model, and validation data, which are not used to determine the free parameters but are used to assess the accuracy.

The validation MSLE can be used to compare the accuracy of the Neural Net (NN), Linear Regression (LR) and Non-Linear Regression (NLR). The Decision Tree (DT) and Neural Network trained directly on the Mpemba Effect (NN2) cannot be compared because they minimize different loss function.

The positive and negative validation accuracies are also computed. These are calculated by predicting whether the Mpemba Effect occurs for randomly selected J , h , N , and two temperatures. The positive accuracy is the percentage of cases where the method predicts the Mpemba Effect in which the effect actually occurs. The negative accuracy is the percentage of times the method correctly predicts that the effect does not occur. As discussed in Sec. III C, the accuracy is meaningless for LR.

For each method, the accuracy increases and the error decreases as the amount of data increases, however it eventually reaches a point at which additional data does not improve the predictions. Tab. II gives the calculations for the four methods for various numbers of data points.

The negative accuracy listed in the table for all four methods is much larger than the positive accuracy. This can be explained by the fact that the Mpemba Effect occurs in approximately 2% of cases. Methods are more likely to minimize a loss function by predicting that the effect does not occur. For reference, a method that always predicts that the effect does not occur regardless of training data, would have a 0% positive accuracy and approximately 98% negative accuracy.

We find that for large data sets, NN2 is most accurate, though NN is almost as accurate and has the added benefit of predicting more information. For very small training sets, NLR is the most effective method at predicting $|a_2|$, although it fails to reach a high level of accuracy with larger data sets.

B. Extrapolation

In the previous section, the parameters for the validation data were different from those of the training data but they were generated in the same range. Machine learning can also be used to extrapolate by validating the model with data in a different range. This is particularly beneficial if the models can make accurate predictions on systems that are more computationally expensive than the systems they are trained on. Out of the parameters N , J , h , and T , only N determines the computational complexity of the calculation. The time to compute $|a_2|$ does not depend on J , h or T .

Fig. 4 plots the positive accuracy of various meth-

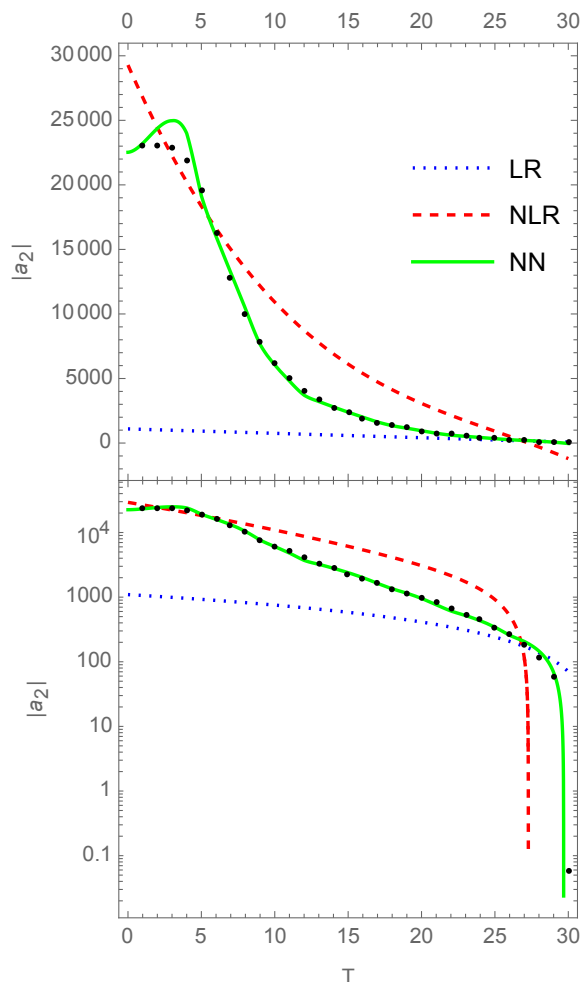


FIG. 3. An example of $|a_2|$ as a function of temperature. The black dots show the actual calculations compared with the predictions for various methods (colored curves). This occurs for $N = 7.$, $J = -6.37$, $h = 0.381$. The upper row gives a linear axis and the lower row gives a log-axis to show behavior at different orders of magnitude. The NN gives the most accurate prediction followed by NLR and then LR. Note that the models are fit not to this data but to a large set of data including various N , J , h , and T .

Training Data Points	DT	NN	NN2	LR	NLR
Error					
100	-	3.1462	-	4.8564	2.4372
1000	-	0.5716	-	4.0791	1.6486
10000	-	0.0522	-	4.0482	1.7776
50000	-	0.0278	-	4.1359	1.6653
200000	-	0.0274	-	4.0256	1.7006
Positive Accuracy					
100	0.0059	0.1323	0.6667	-	0.2235
1000	0.3014	0.1406	0.6140	-	0.1508
10000	0.4599	0.6492	0.8294	-	0.1615
50000	0.6399	0.8351	0.9704	-	0.1894
200000	0.6595	0.7318	0.8603	-	0.1937
Negative Accuracy					
100	0.9816	0.8959	0.9880	-	0.8200
1000	0.9985	0.9924	0.9929	-	0.8898
10000	0.9982	0.9970	0.9947	-	0.8895
50000	0.9972	0.9963	0.9953	-	0.8869
200000	0.9979	0.9974	0.9978	-	0.8849

TABLE II. The error and accuracy for several machine learning methods for varying numbers of training data points. The error is calculated with the MSLE on validation data. The positive/negative accuracy are the fraction of correct results when the method predicts that the effect occurs/does not occur.

ods for predicting the Mpemba Effect in the case when $N = 15$, when it has only been trained on data with $N < 15$. The full results are given in Tab. V in the Appendix. The lines shown in Fig. 4 give a rough approximation for how the accuracy depends on the maximum parameter excluded. Uncertainties are given by the standard deviation of 5 re-samples.

When values of N close to 15 are included in the training data, the neural networks are once again the most accurate methods, however, the DT is relatively accurate at making predictions even when only $N = 5$ is included. In fact, changing which values of N are included has very little impact on the accuracy of the predictions, indicating that N has very little effect in the prediction with this algorithm. These results agree with the crude prediction from the correlation coefficients, given in Tab. I.

It is reasonable to assume that the methods that are best at long range extrapolation in the ranges we consider will also be most effective at long range extrapolation outside the range we consider or for different systems than the Ising model. However, this has not been demonstrated for certain and merits further investigation.

Long range extrapolation could be useful due to the high computational cost for a_2 for higher N . The number of states for a given N is 2^N , leading to a $2^N \times 2^N$ transition matrix. The computational cost of the eigenvalues for a $M \times M$ matrix is $\mathcal{O}(M^2)$ [41]. Thus the computational cost for calculating a_2 is 2^{2N} . Thus, a calculation with $N = 5$ is quicker than a calculation with $N = 15$ by a factor of 2^{20} . Accurate prediction trained on much simpler systems could save considerable computational cost.

	TME	ME
Positive accuracy	0.7764 ± 0.064	0.3035 ± 0.134
Negative accuracy	0.8487 ± 0.070	0.9848 ± 0.012

TABLE III. The predictions for the Mpemba Effect when the neural network is only trained on data where the Mpemba Effect is not present. The neural network is trained on 20000 data points.

Notably, the Mpemba Effect can be predicted even if it is trained only with data in which it does not occur. Results for this extrapolation are given in Tab. III. The first prediction of the Mpemba Effect (ME) is the same as in the previous sections. The second method of prediction, referred to as the Total Mpemba Effect (TME), measures the accuracy of predicting whether or not the Mpemba Effect occurs for any temperature for a given J , h , and N .

C. The Strong Mpemba Effect

In addition to the Mpemba Effect, machine learning methods can be used to predict the Strong Mpemba Effect, defined in Ref. [11]. In this situation, the hot system cools exponentially faster than the cold system.

The Strong Mpemba effect occurs when $a_2 = 0$ and $T \neq T_b$. The neural network is trained on three input variables, N , J , and h . The output is 1 if the strong Mpemba Effect occurs for any temperature; the output is 0 if the Strong Mpemba Effect does not occur. Results are given in Tab. IV.

Positive accuracy	Negative Accuracy
0.4633 ± 0.043	0.995 ± 0.0016

TABLE IV. The validation accuracy for the Strong Mpemba Effect. It is trained with 20000 data points.

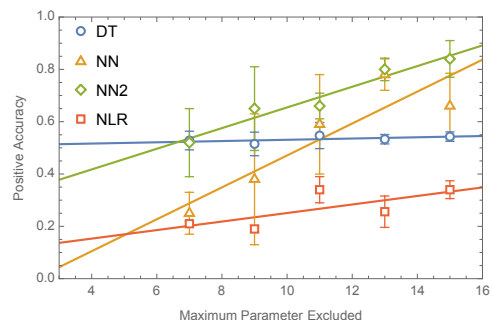


FIG. 4. A plot of the positive accuracy vs. maximum value of N excluded. The full data is given in Tab. V. Best fit lines are shown to roughly estimate the relationship between the variables

V. CONCLUSION

The Mpemba Effect has been shown to occur in many systems, beyond the freezing of water. It has been shown to have applications in quantum heat engines. These applications motivate better predictions of the effect.

In order to understand this effect, this work applies statistical methods to the Mpemba Effect in the Ising model. We demonstrate that a number of machine learning methods can be used. Neural networks are the most effective method when a large enough training data set is used. For very small data sets, non-linear regression with the LASSO method may be more effective at predicting a_2 . These methods can predict the Mpemba Effect in systems much more complex than those on which they were trained. The decision tree method may be the most effective method at making predictions far outside the range it was trained on. Additionally, the Mpemba Effect can

be predicted with neural networks when it is trained only on data where the Mpemba Effect does not occur. This indicates that information about the Mpemba Effect exists in situations in which it does not occur. Finally, we demonstrate that the strong Mpemba Effect can also be predicted using machine learning methods.

These predictions were performed for the Mpemba Effect in the Ising model, however, the relative accuracy of each method might hold for the Mpemba Effect in other systems. Determination of the accuracy of various methods in other systems merits further investigation.

Acknowledgments — This work was funded by an Ave Maria University undergraduate research grant by Michael and Lisa Schwartz. Thanks to Tomás Licheri for completing crucial tasks necessary for this research.

-
- [1] E B Mpemba and D G Osborne, “Cool?” *Physics Education* **4**, 172–175 (1969).
- [2] Aristotle, *Metaphysics*, edited by Translated by W. D. Ross (The Internet Classics Archive, 350BCE).
- [3] Francis Bacon, *The Novum Organum of Sir Francis Bacon* (Printed for Thomas Lee London, 1677) pp. [3], 32 p.
- [4] Henry C. Burridge and F. Paul Linden, “Questioning the mpemba effect: hot water does not cool more quickly than cold,” *Sci. Rep.* **6** (2016), <https://doi.org/10.1038/srep37665>.
- [5] Antonio Lasanta, Francisco Vega Reyes, Antonio Prados, and Andrés Santos, “When the hotter cools more quickly: Mpemba effect in granular fluids,” *Phys. Rev. Lett.* **119**, 148001 (2017).
- [6] Marco Baity-Jesi, Enrico Calore, Andres Cruz, Luis Antonio Fernandez, José Miguel Gil-Narvi6n, Antonio Gordillo-Guerrero, David I6niguez, Antonio Lasanta, Andrea Maiorano, Enzo Marinari, Victor Martin-Mayor, Javier Moreno-Gordo, Antonio Mu6noz Sudupe, Denis Navarro, Giorgio Parisi, Sergio Perez-Gaviro, Federico Ricci-Tersenghi, Juan Jesus Ruiz-Lorenzo, Sebastiano Fabio Schifano, Beatriz Seoane, Alfonso Taranc6n, Raffaele Tripiccione, and David Yllanes, “The mpemba effect in spin glasses is a persistent memory effect,” *Proceedings of the National Academy of Sciences* **116**, 15350–15355 (2019).
- [7] Aurora Torrente, Miguel A. L6pez-Casta6o, Antonio Lasanta, Francisco Vega Reyes, Antonio Prados, and Andr6s Santos, “Large mpemba-like effect in a gas of inelastic rough hard spheres,” *Physical Review E* **99** (2019), [10.1103/physreve.99.060901](https://doi.org/10.1103/physreve.99.060901).
- [8] A. Gij6n, A. Lasanta, and E. R. Hern6ndez, “Paths towards equilibrium in molecular systems: The case of water,” *Physical Review E* **100** (2019), [10.1103/physreve.100.032103](https://doi.org/10.1103/physreve.100.032103).
- [9] Alberto Megias and Andr6s Santos, “Mpemba-like effect protocol for granular gases of inelastic and rough hard disks,” (2022).
- [10] Zhiyue Lu and Oren Raz, “Nonequilibrium thermodynamics of the markovian mpemba effect and its inverse,” *Proceedings of the National Academy of Sciences* **114**, 5083–5088 (2017).
- [11] Israel Klich, Oren Raz, Ori Hirschberg, and Marija Vucelja, “Mpemba index and anomalous relaxation,” *Phys. Rev. X* **9**, 021060 (2019).
- [12] Daniel Busiello, Deepak Gupta, and Amos Maritan, “Inducing and optimizing markovian mpemba effect with stochastic reset,” *New Journal of Physics* **23** (2021), [10.1088/1367-2630/ac2922](https://doi.org/10.1088/1367-2630/ac2922).
- [13] Gianluca Teza, Ran Yaacoby, and Oren Raz, “Relaxation shortcuts through boundary coupling,” (2021).
- [14] Zhiqiang Tang, Weidong Huang, Yagang Zhang, Yanxia Liu, and Lin Zhao, “Direct observation of the mpemba effect with water: Probe the mysterious heat transfer,” *InfoMat* (2022), [10.1002/inf2.12352](https://doi.org/10.1002/inf2.12352).
- [15] Monwhea Jeng, “The mpemba effect: When can hot water freeze faster than cold?” *American Journal of Physics* **74**, 514–522 (2006).
- [16] P Chaddah, S Dash, Kranti Kumar, and A Banerjee, “Overtaking while approaching equilibrium,” arXiv preprint arXiv:1011.3598 (2010).
- [17] Fabian Schwarzendahl and Hartmut L6wen, “Anomalous cooling and overcooling of active systems,” (2021).
- [18] Alberto Megias, Andres Santos, and Antonio Prados, “Thermal versus entropic mpemba effect in molecular gases with nonlinear drag,” *Physical Review E* **105** (2022), [10.1103/PhysRevE.105.054140](https://doi.org/10.1103/PhysRevE.105.054140).
- [19] Apurba Biswas, Prasad v v, and R. Rajesh, “Mpemba effect in anisotropically driven inelastic maxwell gases,” *Journal of Statistical Physics* **186** (2022), [10.1007/s10955-022-02891-w](https://doi.org/10.1007/s10955-022-02891-w).
- [20] Jan Meibohm, Danilo Forastiere, Tunrayo Adeleke-Larodo, and Karel Proesmans, “Relaxation-speed crossover in anharmonic potentials,” *Physical Review E* **104** (2021), [10.1103/PhysRevE.104.L032105](https://doi.org/10.1103/PhysRevE.104.L032105).
- [21] Yun-Ho Ahn, Hyery Kang, Dong-Yeun Koh, and Huen Lee, “Experimental verifications of mpemba-like behaviors of clathrate hydrates,” *Korean Journal of Chemical Engineering* **33**, 1903–1907 (2016).

- [22] P Alex Greaney, Giovanna Lani, Giancarlo Cicero, and Jeffrey C Grossman, “Mpemba-like behavior in carbon nanotube resonators,” *Metallurgical and Materials Transactions A* **42**, 3907–3912 (2011).
- [23] A. Gal and O. Raz, “Precooling strategy allows exponentially faster heating,” *Phys. Rev. Lett.* **124**, 060602 (2020).
- [24] Raphaël Chétrite, Avinash Kumar, and John Bechhoefer, “The metastable mpemba effect corresponds to a non-monotonic temperature dependence of extractable work,” *Frontiers in Physics* **9** (2021), 10.3389/fphy.2021.654271.
- [25] Jie Lin, Kai Li, Jizhou He, Jie Ren, and Jianhui Wang, “Power statistics of otto heat engines with the mpemba effect,” *Phys. Rev. E* **105**, 014104 (2022).
- [26] Andrei Militaru, Antonio Lasanta, Martin Frimmer, Luis Bonilla, Lukas Novotny, and Raúl Rica, “Kovacs memory effect with an optically levitated nanoparticle,” *Physical Review Letters* **127** (2021), 10.1103/PhysRevLett.127.130603.
- [27] E. Mompó, Miguel Ángel López-Castaño, Antonio Lasanta, Francisco Reyes, and Aurora Torrente, “Memory effects in a gas of viscoelastic particles,” *Physics of Fluids* **33**, 062005 (2021).
- [28] Isidoro Pemartín, Emanuel Mompó, Antonio Lasanta, Víctor Martín-Mayor, and Jesús Salas, “Slow growth of magnetic domains helps fast evolution routes for out-of-equilibrium dynamics,” (2021).
- [29] Antonio Patrón Castro, Bernardo Sánchez-Rey, and Antonio Prados, “Universal non-exponential relaxation and memory effects in a fluid with non-linear drag,” (2021).
- [30] Vuk Uskokovic, “. . .and all the world a dream: Memory effects outlining the path to explaining the strange temperature-dependency of crystallization of water, a.k.a. the mpemba effect,” **4**, 59 – 117 (2020).
- [31] Nicholas Walker, Ka-Ming Tam, and Mark Jarrell, “Deep learning on the 2-dimensional ising model to extract the crossover region with a variational autoencoder,” *Scientific Reports* **10** (2020), 10.1038/s41598-020-69848-5.
- [32] Alan Morningstar and Roger G. Melko, “Deep learning the ising model near criticality,” (2017), 10.48550/ARXIV.1708.04622.
- [33] Nataliya Portman and Isaac Tamblyn, “Sampling algorithms for validation of supervised learning models for ising-like systems,” *Journal of Computational Physics* **350**, 871–890 (2017).
- [34] Walter Edwin Arnoldi, “The principle of minimized iterations in the solution of the matrix eigenvalue problem,” *Quarterly of applied mathematics* **9**, 17–29 (1951).
- [35] Leo Breiman, Jerome H. Friedman, Richard Olshen, and Charles Stone, *Classification and Regression Trees*, CART (Wadsworth and Brooks, Monterey, CA, 1984).
- [36] Timothy O. Hodson, Thomas M. Over, and Sydney S. Foks, “Mean squared error, deconstructed,” *Journal of Advances in Modeling Earth Systems* **13**, e2021MS002681 (2021), e2021MS002681 2021MS002681.
- [37] Robert Tibshirani, “Regression shrinkage and selection via the lasso,” *Journal of the Royal Statistical Society. Series B (Methodological)* **58**, 267–288 (1996).
- [38] Baptiste Guegan, John Hardin, Justin Stevens, and Mike Williams, “Model selection for amplitude analysis,” *JINST* **10**, P09002 (2015), arXiv:1505.05133 [physics.data-an].
- [39] D. Sadasivan, M. Mai, and M. Döring, “S- and p-wave structure of $S = -1$ meson-baryon scattering in the resonance region,” *Phys. Lett. B* **789**, 329–335 (2019), arXiv:1805.04534 [nucl-th].
- [40] J. Landay, M. Mai, M. Döring, H. Habertzettl, and K. Nakayama, “Towards the Minimal Spectrum of Excited Baryons,” *Phys. Rev. D* **99**, 016001 (2019), arXiv:1810.00075 [nucl-th].
- [41] William H. Press, Saul A. Teukolsky, William T. Vetterling, and Brian P. Flannery, *Numerical Recipes in C*, 2nd ed. (Cambridge University Press, Cambridge, USA, 1992).

Appendix A: Additional Data

In this section we give data for reference that is not used in the main analysis and discussion of the paper. Tab. V gives the extrapolation accuracy of the methods. Positive accuracies of this table are plotted in Fig. 4 and the format is equivalent to Tab. II.

Excluded Values of N	DT	NN	NN2	NLR
		Positive Accuracy		
15	0.543658 ± 0.01865	0.663848 ± 0.12557	0.842167 ± 0.072441	0.343563 ± 0.0304734
13,15	0.533428 ± 0.018449	0.779604 ± 0.063325	0.804049 ± 0.0434704	0.256295 ± 0.0626766
11,13,15	0.547965 ± 0.050374	0.592272 ± 0.199423	0.661132 ± 0.0495233	0.346793 ± 0.0520674
9,11,13,15	0.515566 ± 0.0450916	0.382676 ± 0.256134	0.647258 ± 0.164046	0.190974 ± 0.0138648
7,9,11,13,15	0.528393 ± 0.035632	0.274173 ± 0.0840219	0.522212 ± 0.128876	0.218488 ± 0.00901212
		Negative Accuracy		
15	0.996207 ± 0.00245	0.99723 ± 0.000954173	0.997952 ± 0.00042289	0.718728 ± 0.0392236
13,15	0.99757 ± 0.001162	0.992953 ± 0.00388419	0.996802 ± 0.00108171	0.83444 ± 0.04182
11,13,15	0.998175 ± 0.000508	0.987025 ± 0.00648745	0.997013 ± 0.000912489	0.890572 ± 0.0353344
9,11,13,15	0.996978 ± 0.001237	0.958839 ± 0.0328791	0.996679 ± 0.00173007	0.837763 ± 0.034161
7,9,11,13,15	0.99767 ± 0.00033	0.960547 ± 0.0529037	0.992296 ± 0.01823	0.93159 ± 0.00735792

TABLE V. Extrapolation accuracy. The data is trained on 50,000 data points.

c_{0000}	12.0493	c_{0001}	56.5418	c_{0002}	-77.7456	c_{0003}	-3.88612	c_{0004}	4.93836
c_{0011}	11.9538	c_{0012}	-389.284	c_{0013}	-12.5517	c_{0014}	-6.88152	c_{0023}	4.51196
c_{0024}	0.37328	c_{0034}	0.780776	c_{0044}	67.0015	c_{0111}	-11.4937	c_{0112}	-77.7841
c_{0113}	-5.35089	c_{0114}	-1.60171	c_{0221}	-308.538	c_{0222}	-11.4937	c_{0224}	87.8123
c_{0331}	-801.778	c_{0332}	67.5452	c_{0333}	458.608	c_{0334}	183.366	c_{0441}	335.435
c_{0442}	-418.124	c_{0443}	37.4534	c_{0444}	-38.2862	c_{0123}	-0.00109161	c_{0124}	16.838
c_{0134}	0.431855	c_{0234}	0.00739725	c_{1114}	0.294404	c_{3334}	-16.9157	c_{4441}	-193.343

TABLE VI. LASSO parameters for a fit with 500000 data points. Fit parameters, $c_{k_1 k_2 k_3 k_4}$ are given in Eq. (12). All parameters not present in this table are either excluded by the LASSO as described in the main text or unnecessary because they are multiplied by a term identical to that of one an included parameter.

Tab. VI gives the best fit parameters for non-linear regression. Parameters not included in the table are either mathematically identical to an excluded parameter or shown by the LASSO method to have less impact. The fit was performed with 50000 data points and corresponds to the fifth row of each section of Tab. II for NLR, however, NLR for any amount of data points greater than 1000 had similar minima. Note that the fit was done to data with $|a_2|$ multiplied by a factor of 10000 as described in the text. To relate these results to data that has not been prepared in this way, one should divide each parameter by 10000.